ELSEVIER
IFAC
PUBLICATIONS
www.elsevier.com/locate/ifac

LINE-OF-SIGHT PATH FOLLOWING OF UNDERACTUATED MARINE CRAFT

Thor I. Fossen *,[1] **Morten Breivik** * **Roger Skjetne** *

* *Centre of Ships and Ocean Structures (CESOS), Norwegian University of Science and Technology (NTNU), NO-7491 Trondheim, Norway. E-mails: tif@itk.ntnu.no, mortebre@itk.ntnu.no, skjetne@ieee.org*

Abstract: A 3 degrees of freedom (surge, sway, and yaw) nonlinear controller for path following of marine craft using only two controls is derived using nonlinear control theory. Path following is achieved by a geometric assignment based on a line-of-sight projection algorithm for minimization of the cross-track error to the path. The desired speed along the path can be specified independently. The control laws in surge and yaw are derived using backstepping. This results in a dynamic feedback controller where the dynamics of the uncontrolled sway mode enters the yaw control law. UGAS is proven for the tracking error dynamics in surge and yaw while the controller dynamics is bounded. A case study involving an experiment with a model ship is included to demonstrate the performance of the controller and guidance systems. *Copyright ©2003 IFAC.*

Keywords: Ship steering, Line-of-Sight guidance, Path following, Maneuvering, Nonlinear control, Underactuated control, Experimental results

1. INTRODUCTION

In many applications offshore it is of primary importance to steer a ship, a submersible or a rig along a desired *path* with a prescribed *speed* (Fossen 1994, 2002). The path is usually defined in terms of *way-points* using the *Cartesian* coordinates $(x_k, y_k) \in \mathbb{R}^2$. In addition, each way-point can include turning information usually specified by a circle arc connecting the way-point before and after the way-point of interest. Desired vessel speed $u_d \in \mathbb{R}$ is also associated with each way-point implying that the speed must be changed along the path between the way-points. The path following problem can be formulated as two control objectives (Skjetne *et al.* 2002). The first objective is to reach and follow a desired path (x_d, y_d). This is referred to as the *geometric assignment*. In this paper a *line-of-sight* (LOS) projection algorithm is used for this purpose. The desired geometric path consists of straight line segments connected by way-points. The second control objective, *speed assignment*, is defined in terms of a prescribed speed u_d along the body-fixed x-axis of the ship. This speed will be identical to the path speed once the ship has converged to the path. Hence, the desired speed profile can be assigned dynamically.

1.1 Control of Underactuated Ships

For floating rigs and supply vessels, trajectory tracking in *surge*, *sway*, and *yaw* (3 DOF) is easily achieved since independent control forces and moments are simultaneously available in all degrees of freedom. For slow speed, this is referred to as dynamic positioning (DP) where the ship is controlled by means of tunnel thrusters, azimuths, and main propellers; see Fossen (2002). Conventional ships, on the other hand, are usually equipped with one or two main propellers for forward speed control and rudders for turning control.

[1] Supported by the Norwegian Research Council through the Centre of Ships and Ocean Structures, Centre of Excellence at NTNU.

The minimum configuration for way-point tracking control is one main propeller and a single rudder. This means that only two controls are available, thus rendering the ship underactuated for the task of 3 DOF tracking control.

Recently, underactuated tracking control in 3 DOF has been addressed by Pettersen and Nijmeijer (1999, 2001), Jiang and Nijmeijer (1999), Sira-Ramirez (1999), Jiang (2002), Do *et al.* (2002), and Lefeber *et al.* (2003). These designs deals with simultaneous tracking control in all three modes (x, y, ψ) using only two controls. One of the main problems with this approach is that integral action, needed for compensation of slowly-varying disturbances due to wind, waves, and currents, can only be assigned to two modes (surge and yaw); see Pettersen and Fossen (2000). Consequently, robustness to environmental disturbances is one limiting factor for these methods. In addition, requirements for a persistently exciting reference yaw velocity results in unrealistic topological restrictions on which type of paths that can be tracked by these controllers (Lefeber *et al.* 2003).

Conventional way-point guidance systems are usually designed by reducing the output space from 3 DOF position and heading to 2 DOF heading and surge (Healey and Marco 1992). In its simplest form this involves the use of a classical autopilot system where the commanded yaw angle ψ_d is generated such that the *cross-track error* is minimized. This can be done in a multivariable controller, for instance $\mathcal{H}_\infty$ or LQG, or by including an additional tracking error control-loop in the autopilot; see Holzhüter and Schultze (1996), and Holzhüter (1997). A path following control system is usually designed such that the ship moves forward with reference speed u_d at the same time as the cross-track error to the path is minimized. As a result, ψ_d and u_d are tracked using only two controls. The desired path can be generated using a route management system or by specifying way-points (Fossen 2002). If weather data are available, the optimal route can be generated such that the effects of wind and water resistance are minimized.

1.2 Main Contribution

The main contribution of this paper is a ship maneuvering design involving a LOS guidance system and a nonlinear feedback tracking controller. The desired output is reduced from (x_d, y_d, ψ_d) to ψ_d and u_d using a LOS projection algorithm. The tracking task $\psi(t) \to \psi_d(t)$ is then achieved using only one control (normally the rudder), while tracking of the speed assignment u_d is performed by the remaining control (the main propeller). Since we are dealing with segments of straight lines, the LOS projection algorithm will guarantee that the task of path following is satisfied.

First, a LOS guidance procedure is derived. This includes a projection algorithm and a way-point switching algorithm. To avoid large bumps in ψ_d when switching, and to provide the necessary derivatives of ψ_d to the controller, the commanded LOS heading is fed through a reference model. Secondly, a nonlinear 2 DOF tracking controller is derived using the backstepping technique. Three stabilizing functions $\alpha = [\alpha_1, \alpha_2, \alpha_3]^\top$ are defined where α_1 and α_3 are specified to satisfy the tracking objectives in the controlled surge and yaw modes. The stabilizing function α_2 in the uncontrolled sway mode is left as a free design variable. By assigning dynamics to α_2, the resulting controller becomes a dynamic feedback controller so that $\alpha_2(t) \to v(t)$ (sway velocity) during path following. This is a new idea that adds to the extensive theory of backstepping. The presented design technique results in a robust controller for underactuated ships since integral action can be implemented for both path following and speed control.

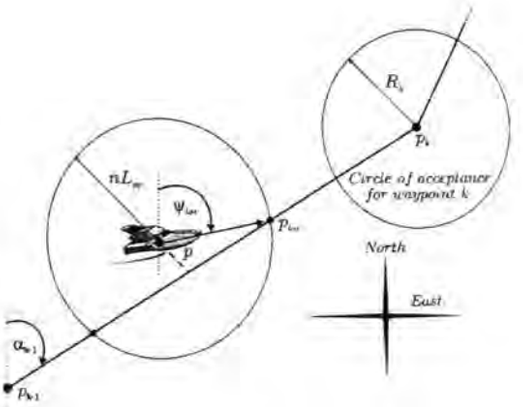

Fig. 1. The Line-of-Sight guidance principle.

1.3 Problem Statement

The problem statement is stated as a maneuvering problem with the following two objectives (Skjetne *et al.* 2002):

LOS Geometric Task: Force the vessel position $p = [x, y]^\top$ to converge to a desired path by forcing the yaw angle ψ to converge to the LOS angle:

$$\psi_{\text{los}} = \text{atan2}\left(y_{\text{los}} - y, x_{\text{los}} - x\right) \tag{1}$$

where the LOS position $p_{\text{los}} = [x_{\text{los}}, y_{\text{los}}]^\top$ is the point along the path which the vessel should be pointed at; see Figure 1. Note that utilizing the four quadrant inverse tangent function atan2(y, x) ensures the mapping $\psi_{\text{los}} \in \langle -\pi, \pi \rangle$.

Dynamic Task: Force the speed u to converge to a desired speed assignment u_d, that is:

$$\lim_{t \to \infty} [u(t) - u_d(t)] = 0 \tag{2}$$

where u_d is the desired speed composed along the body-fixed x-axis.

2. LINE-OF-SIGHT GUIDANCE SYSTEM

The desired geometric path considered here is composed by a collection of way-points in a way-point

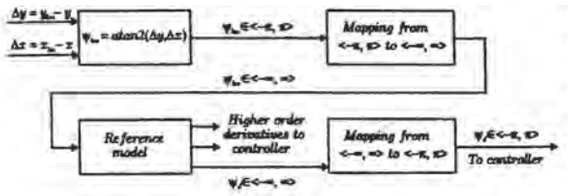

Fig. 2. LOS guidance system.

table. The LOS position p_{los} is located somewhere along the straight line segment connecting the previous p_{k-1} and current p_k way-points. Let the ship's current horizontal position p be the center of a circle with radius of n ship lengths (nL_{pp}). This circle will intersect the current straight line segment at two points where p_{los} is selected as the point closest to the next way-point. To calculate p_{los}, two equations with two unknowns must be solved online. These are:

$$(y_{\text{los}} - y)^2 + (x_{\text{los}} - x)^2 = (nL_{pp})^2 \quad (3)$$

$$\frac{y_{\text{los}} - y_{k-1}}{x_{\text{los}} - x_{k-1}} = \frac{y_k - y_{k-1}}{x_k - x_{k-1}} = \tan(\alpha_{k-1}) \quad (4)$$

The first equation is recognized as the theorem of *Pythagoras*, while the second equation states that the slope of the path between the previous and current way-point is constant.

Selecting way-points in the way-point table relies on a switching algorithm. A criteria for selecting the next way-point, located at $p_{k+1} = [x_{k+1}, y_{k+1}]^\top$, is for the ship to be within a *circle of acceptance* of the current way-point p_k. Hence, if at some instant of time t the ship position $p(t)$ satisfies:

$$(x_k - x(t))^2 + (y_k - y(t))^2 \leq R_k^2, \quad (5)$$

the next way-point is selected from the way-point table. R_k denotes the radius of the circle of acceptance for the current way-point. It is imperative that the circle enclosing the ship has a sufficient radius such that the solutions to (3) exist. Therefore, $nL_{pp} \geq R_k$, for all k is a necessary bound.

The signals ψ_d, $\dot{\psi}_d$, and $\ddot{\psi}_d$ are required by the controller. To provide these signals, a reference model is implemented. This will generate the necessary signals as well as smoothing the discontinuous way-point switching to prevent rapid changes in the desired yaw angle fed to the controller. However, since the atan2-function is discontinuous at the $-\pi/\pi$-junction, the reference model cannot be applied directly to its output. This is solved by constructing a mapping $\Psi_d : \langle -\pi, \pi \rangle \rightarrow \langle -\infty, \infty \rangle$ and sandwiching the reference filter between Ψ_d and Ψ_d^{-1}; see Fig. 2. Details about the mappings can be found in Breivik (2003).

3. LINE-OF-SIGHT CONTROL DESIGN

A conventional tracking control system for 3 DOF is usually implemented using a standard PID autopilot in series with a LOS algorithm as shown in Figure 3. Hence, a state-of-the-art autopilot system can be modified to take the LOS reference angle as input. This adds flexibility since the default commercial autopilot system of the ship can be used together with the LOS guidance system. The speed can be adjusted manually by the Captain or automatically using the path speed profile. A model-based nonlinear controller that solves the control objective as stated in Section 1.3 is derived next. The basis is a 3 DOF ship maneuvering model.

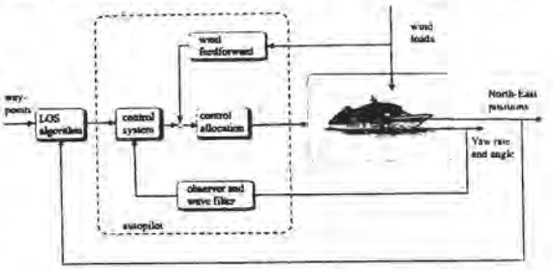

Fig. 3. Conventional autpilot with a LOS projection algorithm for way-point tracking.

3.1 Surge, Sway, and Yaw Equations of Motion

Consider the 3 DOF nonlinear maneuvering model in the form (Fossen 2002):

$$\dot{\eta} = R(\psi)\nu \quad (6)$$

$$M\dot{\nu} + N(\nu)\nu = \begin{bmatrix} \tau_1 \\ 0 \\ \tau_3 \end{bmatrix} \quad (7)$$

where $\eta = [x, y, \psi]^\top$, $\nu = [u, v, r]^\top$ and:

$$R(\psi) = \begin{bmatrix} \cos\psi & -\sin\psi & 0 \\ \sin\psi & \cos\psi & 0 \\ 0 & 0 & 1 \end{bmatrix} \quad (8)$$

The matrices M and N are defined as:

$$M = \begin{bmatrix} m_{11} & 0 & 0 \\ 0 & m_{22} & m_{23} \\ 0 & m_{32} & m_{33} \end{bmatrix}$$

$$= \begin{bmatrix} m - X_{\dot{u}} & 0 & 0 \\ 0 & m - Y_{\dot{v}} & mx_g - Y_{\dot{r}} \\ 0 & mx_g - N_{\dot{v}} & I_z - N_{\dot{r}} \end{bmatrix}$$

$$N(\nu) = \begin{bmatrix} n_{11} & 0 & 0 \\ 0 & n_{22} & n_{23} \\ 0 & n_{32} & n_{33} \end{bmatrix} = \begin{bmatrix} -X_u & 0 & 0 \\ 0 & -Y_v & mu - Y_r \\ 0 & -N_v & mx_g u - N_r \end{bmatrix}$$

Symmetrization of the System Inertia Matrix: If $M \neq M^\top$, the inertia matrix can be made symmetric by acceleration feedback; see Fossen *et al.* (2002) and Lindegaard (2003). This is necessary in a Lyapunov stability analysis for a kinetic energy function to be applied. For low-speed applications like DP, a symmetric system inertia matrix M is an accurate assumption. However, for craft operating at high speed, this assumption is not valid since M is largely nonsymmetric due to hydrodynamically added mass.

Acceleration feedback is implemented by the inner feedback loop:

$$\tau_3 = (m_{32} - m_{23})\dot{v} + \tau_3^* \quad (9)$$

where the sway acceleration $\dot{v}$ is assumed to be measured. The new control variable τ_3^* is then used for maneuvering control. The resulting model is:

$$\dot{\eta} = R(\psi)\nu \tag{10}$$

$$M^*\dot{\nu} + N(\nu)\nu = \begin{bmatrix} \tau_1 \\ 0 \\ \tau_3^* \end{bmatrix} \tag{11}$$

where

$$M^* = \begin{bmatrix} m_{11} & 0 & 0 \\ 0 & m_{22} & m_{23} \\ 0 & m_{23} & m_{33} \end{bmatrix} = (M^*)^\top > 0 \tag{12}$$

Consequently, the following control design can be based on a symmetric representation of M.

3.2 Control Design

The design is based on the model (6)–(7) where M is symmetric or at least made symmetric by acceleration feedback. Define the error signals $z_1 \in \mathbb{R}$ and $z_2 \in \mathbb{R}^3$ according to:

$$z_1 \triangleq \psi - \psi_d \tag{13}$$

$$z_2 \triangleq [z_{2,1}, z_{2,2}, z_{2,3}]^\top = \nu - \alpha \tag{14}$$

where ψ_d and its derivatives are provided by the guidance system, $u_d \in \mathcal{L}_\infty$ is the desired speed, and $\alpha = [\alpha_1, \alpha_2, \alpha_3]^\top \in \mathbb{R}^3$ is a vector of stabilizing functions to be specified later. Next, let:

$$h = [0, 0, 1]^\top \tag{15}$$

such that:

$$\begin{aligned} \dot{z}_1 &= r - r_d = h^\top \nu - r_d \\ &= \alpha_3 + h^\top z_2 - r_d \end{aligned} \tag{16}$$

where $r_d = \dot{\psi}_d$ and:

$$M\dot{z}_2 = M\dot{\nu} - M\dot{\alpha} = \tau - N\nu - M\dot{\alpha}. \tag{17}$$

Motivated by backstepping; see Fossen (2002, Ch. 7), we consider the control Lyapunov function (CLF):

$$V = \frac{1}{2}z_1^2 + \frac{1}{2}z_2^\top M z_2, \qquad M = M^\top > 0. \tag{18}$$

Differentiating V along the trajectories of z_1 and z_2, yields:

$$\begin{aligned} \dot{V} &= z_1\dot{z}_1 + z_2^\top M\dot{z}_2 \\ &= z_1(\alpha_3 + h^\top z_2 - r_d) + z_2^\top(\tau - N\nu - M\dot{\alpha}). \end{aligned}$$

Choosing the virtual control α_3 as:

$$\alpha_3 = -cz_1 + r_d \tag{19}$$

while α_1 and α_2 are yet to be defined, gives:

$$\begin{aligned} \dot{V} &= -cz_1^2 + z_1 h^\top z_2 + z_2^\top(\tau - N\nu - M\dot{\alpha}) \\ &= -cz_1^2 + z_2^\top(hz_1 + \tau - N\nu - M\dot{\alpha}). \end{aligned} \tag{20}$$

Suppose we can assign:

$$\tau = \begin{bmatrix} \tau_1 \\ 0 \\ \tau_3 \end{bmatrix} = M\dot{\alpha} + N\nu - Kz_2 - hz_1 \tag{21}$$

where $K = \mathrm{diag}(k_1, k_2, k_3) > 0$. This results in:

$$\dot{V} = -cz_1^2 - z_2^\top K z_2 < 0, \quad \forall z_1 \neq 0, z_2 \neq 0, \tag{22}$$

and by standard Lyapunov arguments, this guarantees that (z_1, z_2) is bounded and converges to zero.

However, notice from (21) that we can only prescribe values for τ_1 and τ_3, that is:

$$\tau_1 = m_{11}\dot{\alpha}_1 + n_{11}u - k_1(u - \alpha_1)$$

$$\tau_3 = m_{32}\dot{\alpha}_2 + m_{33}\dot{\alpha}_3 + n_{32}v + n_{33}r - k_3(r - \alpha_3) - z_1$$

Choosing $\alpha_1 = u_d$ solves the dynamic task and gives the closed-loop:

$$m_{11}(\dot{u} - \dot{u}_d) + k_1(u - u_d) = 0. \tag{23}$$

in surge. The remaining equation ($\tau_2 = 0$) in (21) results in a dynamic equality constraint:

$$m_{22}\dot{\alpha}_2 + m_{23}\dot{\alpha}_3 + n_{22}v + n_{23}r - k_2(v - \alpha_2) = 0. \tag{24}$$

Substituting $\dot{\alpha}_3 = c^2 z_1 - cz_{2,3} + \dot{r}_d$, $v = \alpha_2 + z_{2,2}$, and $r = \alpha_3(z_1, r_d) + z_{2,3}$ into (24), gives:

$$m_{22}\dot{\alpha}_2 = -n_{22}\alpha_2 + \gamma(z_1, z_2, r_d, \dot{r}_d) \tag{25}$$

where:

$$\begin{aligned} \gamma(z_1, z_2, r_d, \dot{r}_d) = (n_{23}c - m_{23}c^2)z_1 + (k_2 - n_{22})z_{2,2} \\ + (m_{23}c - n_{23})z_{2,3} - m_{23}\dot{r}_d - n_{23}r_d. \end{aligned}$$

The variable α_2 becomes a dynamic state of the controller according to (25). Furthermore, $n_{22} > 0$ implies that (25) is a stable differential equation driven by the converging error signals (z_1, z_2) and the bounded reference signals $(r_d, \dot{r}_d)$. Since $z_{2,2}(t) \to 0$, we get that $|\alpha_2(t) - v(t)| \to 0$ as $t \to \infty$. The main result is summarized by Theorem 1:

Theorem 1. (LOS Path Following). The LOS maneuvering problem for the 3 DOF underactuated vessel model (6)–(7) is solved using the control laws:

$$\tau_1 = m_{11}\dot{u}_d + n_{11}u - k_1(u - u_d)$$

$$\tau_3 = m_{32}\dot{\alpha}_2 + m_{33}\dot{\alpha}_3 + n_{32}v + n_{33}r - k_3(r - \alpha_3) - z_1$$

where $k_1 > 0$, $k_3 > 0$, $z_1 \triangleq \psi - \psi_d$, $z_2 \triangleq [u - u_d, v - \alpha_2, r - \alpha_3]^\top$, and:

$$\alpha_3 = -cz_1 + r_d, \qquad c > 0 \tag{26}$$

$$\dot{\alpha}_3 = -c(r - r_d) + \dot{r}_d. \tag{27}$$

The reference signals u_d, $\dot{u}_d$, ψ_d, r_d, and $\dot{r}_d$ are provided by the LOS guidance system, while α_2 is found by numerical integration of:

$$m_{22}\dot{\alpha}_2 = -n_{22}\alpha_2 + (k_2 - n_{22})z_{2,2} - m_{23}\dot{\alpha}_3 - n_{23}r$$

where $k_2 > 0$. This results in a UGAS equilibrium point $(z_1, z_2) = (0, 0)$, while $\alpha_2 \in \mathcal{L}_\infty$ satisfies:

$$\lim_{t\to\infty} |\alpha_2(t) - v(t)| = 0 \tag{28}$$

Remark 1: Notice that the smooth reference signal $\psi_d \in \mathcal{L}_\infty$ must be differentiated twice to produce r_d and $\dot{r}_d$, while $u_d \in \mathcal{L}_\infty$ must be differentiated once to give $\dot{u}_d$. This is most easily achieved by using reference models represented by low-pass filters; see Fossen (2002), Ch. 5.

Fig. 4. CyberShip 2 in action at the MCLab.

PROOF. The closed-loop equations become:

$$\begin{bmatrix} \dot{z}_1 \\ \dot{z}_2 \end{bmatrix} = \begin{bmatrix} -c & h^\top \\ -M^{-1}h & -M^{-1}K \end{bmatrix} \begin{bmatrix} z_1 \\ z_2 \end{bmatrix} \tag{29}$$

$$m_{22}\dot{\alpha}_2 = -n_{22}\alpha_2 + \gamma(z_1, z_2, r_d, \dot{r}_d). \tag{30}$$

From the Lyapunov arguments (18) and (22), the equilibrium $(z_1, z_2) = (0, 0)$ of the z-subsystem is proved UGAS. Moreover, the unforced α_2-subsystem ($\gamma = 0$) is clearly exponentially stable. Since $(z_1, z_2) \in \mathcal{L}_\infty$ and $(r_d, \dot{r}_d) \in \mathcal{L}_\infty$, then $\gamma \in \mathcal{L}_\infty$. This implies that the α_2-subsystem is input-to-state stable from γ to α_2. This is seen by applying for instance $V_2 = \frac{1}{2}m_{22}\alpha_2^2$ which differentiated along solutions of α_2 gives $\dot{V}_2 \leq -\frac{1}{2}n_{22}\alpha_2^2$ for all $|\alpha_2| \geq \frac{2}{n_{22}}|\gamma(z_1, z_2, r_d, \dot{r}_d)|$. By standard comparison functions, it is straight-forward to show that for all $|\alpha_2(t)| \geq \frac{2}{n_{22}}|\gamma(z_1(t), z_2(t), r_d(t), \dot{r}_d(t))|$ then

$$|\alpha_2(t)| \leq |\alpha_2(0)|\, e^{-\frac{n_{22}}{4}t}. \tag{31}$$

Hence, α_2 converges to the bounded set $\{\alpha_2 : |\alpha_2| \leq \frac{2}{n_{22}}||\gamma(z_1, z_2, r_d, \dot{r}_d)||\}$. Since $z_{2,2}(t) \to 0$ as $t \to \infty$, we get the last limit.

4. CASE STUDY: EXPERIMENT PERFORMED WITH THE CS2 MODEL SHIP

The proposed controller and guidance system were tested out at the *Marine Cybernetics Laboratory* (MCLab) located at the Norwegian University of Science and Technology. MCLab is an experimental laboratory for testing of scale models of ships, rigs, underwater vehicles and propulsion systems. The software is developed by using rapid prototyping techniques and automatic code generation under *Matlab/Simulink*™ and *RT-Lab*™. The target PC onboard the model scale vessels runs the *QNX*™ real-time operating system, while experimental results are presented in real-time on a host PC using *Labview*™.

In the experiment, *CyberShip 2* (CS2) was used. It is a 1:70 scale model of an offshore supply vessel with a mass of 15 kg and a length of 1.255 m. The maximum surge force is approx. 2.0 N, while the maximum yaw moment is about 1.5 Nm. The MCLab tank is $L \times B \times D = 40$ m $\times$ 6.5 m $\times$ 1.5 m.

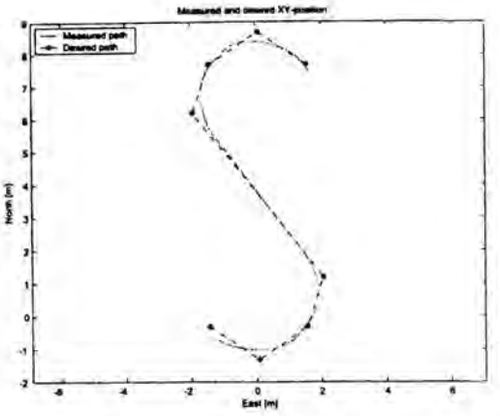

Fig. 5. xy-plot of the measured and desired geometrical path during the experiment.

Figure 4 shows CS2. Three spheres can be seen mounted on the ship, ensuring that its position and orientation can be identified by infrared cameras. Two *Qualisys*™ infrared cameras mounted on a towing carriage currently supply the position and orientation estimates in 6 DOF, but due to a temporary bad calibration, the camera measurements vanished when the ship assumed certain yaw angles and regions of the tank. This affected the results of the experiment and also limited the available space for maneuvering. Nevertheless, good results were obtained. The cameras operate at 10 Hz.

The desired path consists of a total of 8 way-points:

$wpt_1 = (0.372, -0.181)$ $\quad wpt_5 = (6.872, -0.681)$
$wpt_2 = (-0.628, 1.320)$ $\quad wpt_6 = (8.372, -0.181)$
$wpt_3 = (0.372, 2.820)$ $\quad wpt_7 = (9.372, 1.320)$
$wpt_4 = (1.872, 3.320)$ $\quad wpt_8 = (8.372, 2.820)$

representing an S-shape. CS2 was performing the maneuver with a constant surge speed of 0.1 m/s. By assuming equal *Froude numbers*, this corresponds to a surge speed of 0.85 m/s for the full scale supply ship. A higher speed was not attempted because the consequence of vanishing position measurements at higher speed is quite severe. The controller used:

$$M = \begin{bmatrix} 25.8 & 0 & 0 \\ 0 & 33.8 & 1.0115 \\ 0 & 1.0115 & 2.76 \end{bmatrix} \quad N(\nu) = \begin{bmatrix} 2 & 0 & 0 \\ 0 & 7 & 0.1 \\ 0 & 0.1 & 0.5 \end{bmatrix}$$

$$c = 0.75,\ k_1 = 25,\ k_2 = 10,\ k_3 = 2.5$$

In addition, a reference model consisting of three 1st-order low-pass filters in cascade delivered continuos values of ψ_d, r_d, and $\dot{r}_d$. The ship's initial states were:

$$(x_0, y_0, \psi_0) = (-0.69 \text{ m}, -1.25 \text{ m}, 1.78 \text{ rad})$$
$$(u_0, v_0, r_0) = (0.1 \text{ m/s}, 0 \text{ m/s}, 0 \text{ rad/s})$$

Both the ship enclosing circle and the radius of acceptance for all way-points was set to one ship length. Figure 5 shows an xy-plot of the CS2's position together with the desired geometrical path consisting of straight line segments. The ship is seen to follow

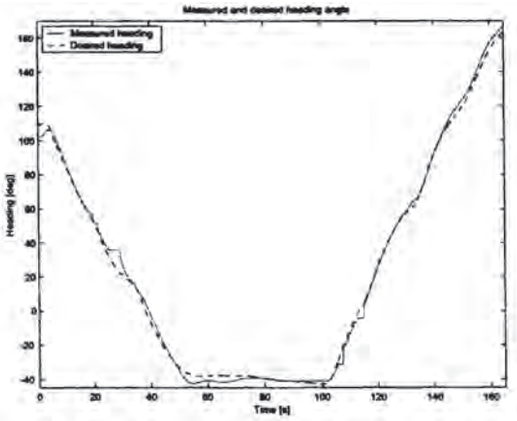

Fig. 6. The actual yaw angle of the ship tracks the desired LOS angle well.

the path very well. To illustrate the effect of the positioning reference system dropping out from time to time, Figure 6 is included. It shows the actual heading angle of CS2 alongside the desired LOS angle. The discontinuities in the actual heading angle is due to the camera measurements dropping out. When the measurements return, the heading angle of the ship is seen to converge nicely to the desired angle.

5. CONCLUSIONS

A nonlinear guidance system that reduces the output space from 3 DOF to 2 DOF was developed by using a LOS projection algorithm. Moreover, a nonlinear controller for maneuvering of underactuated marine craft utilizing dynamic feedback has been developed with a vectorial backstepping approach. UGAS is proven for the controlled error states, and boundedness is proven for a controller dynamic state that will track the sway velocity. The design technique is robust since integral action can easily be implemented. Note that the controller also can be utilized for a fully actuated ship since the control law is derived without assuming a specific control allocation scheme. Hence, the controller and control allocation blocks can be replaced by other algorithms in a modular design. Experiments with a model ship document the performance of the guidance and control systems.

REFERENCES

Breivik, M. (2003). Nonlinear Maneuvering Control of Underactuated Ships. MSc thesis. Dept. of Eng. Cybernetics, Norwegian University of Science and Technology.

Do, K. D., Z. P. Jiang and J. Pan (2002). Underactuated Ship Global Tracking under Relaxed Conditions. *IEEE Transactions on Automatic Control* **TAC-47**(9), 1529–1535.

Fossen, T. I. (1994). *Guidance and Control of Ocean Vehicles*. John Wiley and Sons Ltd. ISBN 0-471-94113-1.

Fossen, T. I. (2002). *Marine Control Systems: Guidance, Navigation and Control of Ships, Rigs and Underwater Vehicles*. Marine Cybernetics AS. Trondheim, Norway. ISBN 82-92356-00-2.

Fossen, T. I., K. P. Lindegaard and R. Skjetne (2002). Inertia Shaping Techniques for Marine Vessels using Acceleration Feedback. In: *Proceedings of the IFAC World Congress*. Elsevier Science. Barcelona.

Healey, A. J. and D. B. Marco (1992). Slow Speed Flight Control of Autonomous Underwater Vehicles: Experimental Results with the NPS AUV II. In: *Proceedings of the 2nd International Offshore and Polar Engineering Conference (ISOPE)*. San Francisco, CA. pp. 523–532.

Holzhüter, T. (1997). LQG Approach for the High-Precision Track Control of Ships. *IEE Proceedings on Control Theory and Applications* **144**(2), 121–127.

Holzhüter, T. and R. Schultze (1996). On the Experience with a High-Precision Track Controller for Commercial Ships. *Control Engineering Practise* **CEP-4**(3), 343–350.

Jiang, Z. P. (2002). Global Tracking Control of Underactuated Ships by Lyapunov's Direct Method. *Automatica* **AUT-38**(2), 301–309.

Jiang, Z.-P. and H. Nijmeijer (1999). A Recursive Technique for Tracking Control of Nonholonomic Systems in Chained Form. *IEEE Transactions on Automatic Control* **TAC-4**(2), 265–279.

Lefeber, A.A.J., K. Y. Pettersen and H. Nijmeijer (2003). Tracking Control of an Underactuated Ship. *IEEE Transactions on Control Systems Technology* **TCST-11**(1), 52–61.

Lindegaard, K.-P. (2003). Acceleration Feedback in Dynamic Positioning Systems. PhD thesis. Department of Engineering Cybernetics, Norwegian University of Science and Technology. Trondheim.

Pettersen, K. Y. and H. Nijmeijer (1999). Tracking Control of an Underactuated Surface Vessel. In: *Proceedings of the IEEE Conference on Decision and Control*. Phoenix, AZ. pp. 4561–4566.

Pettersen, K. Y. and H. Nijmeijer (2001). Underactuated Ship Tracking Control. *International Journal of Control* **IJC-74**, 1435–1446.

Pettersen, K. Y. and T. I. Fossen (2000). Underactuated Dynamic Positioning of a Ship - Experimental Results. *IEEE Transactions on Control Systems Technology* **TCST-8**(5), 856–863.

Sira-Ramirez, H. (1999). On the Control of the Underactuated Ship: A Trajectory Planning Approach. In: *IEEE Conference on Decision and Control*. Phoenix, AZ.

Skjetne, R., T. I. Fossen and P. V. Kokotovic (2002). Output Maneuvering for a Class of Nonlinear Systems. In: *Proc. of the IFAC World Congress*. Barcelona.